NASA/CR-97- 206496

Final Report:

Studies of the Earth Energy Budget and Water Cycle Using Satellite Observations and Model Analyses.

Cooperative Institute for Research in the Atmosphere
Colorado State University

NASA Project NAGW 4122

G.G. Campbell
T.H. Vonder Haar
D.L. Randel
S.Q. Kidder

For the Period September 1, 1994 to August 31, 1997

November 18, 1997

Abstract

During this research period we have utilized the ERBE data set in comparisons to surface properties and water vapor observations in the atmosphere. A relationship between cloudiness and surface temperature anomalies was found. This same relationship was found in a general circulation model, verifying the model. The attempt to construct a homogeneous time series from Nimbus 6, Nimbus 7 and ERBE data is not complete because we are still waiting for the ERBE reanalysis to be completed. It will be difficult to merge the Nimbus 6 data in because its observations occurred when the average weather was different than the other periods, so regression adjustments are not effective.

Introduction

Radiation budget measurements have been made with various instruments over the last 20 years. Here will consider the use of radiation budget observations for climate studies. We attempt the construct a merged time series from the Nimbus 6, Nimbus 7 and ERBE data sets.

Empirical study of the relationship between surface temperature and radiation and cloudiness.

The paper (Appendix A) by Campbell and Vonder Haar summarizes our findings on an empirical comparison of surface temperature and satellite observations. There is a relationship between clouds and surface temperature which could be predictive, but it

predictive, but it explains only a small fraction of the variance of the surface temperature. We hypothesized that more clouds would damp the diurnal cycle so the more cloudy months (than the mean) have a smaller than average difference between temperature maxima and temperature minima. This was confirmed by the observations of ISCCP cloudiness and monthly surface temperature variations. The basic radiative mechanism: clouds shade the surface in the day time, reducing the temperature maxima, and clouds at night warm the minima. The connection to radiation terms: surface radiation budget and ERBE is qualitatively consistent. Not enough variance is explained to be predictive.

Comparing model response to observed response provides a test of the physics included in the general circulation model. Figure 1 shows the sensitivity of surface temperature to clouds and Figure 2 shows a matching plot for the NCAR CCM 2 run with a diurnal cycle. This implies that the model simulates the connection between surface temperature and external radiative perturbations of clouds correctly.

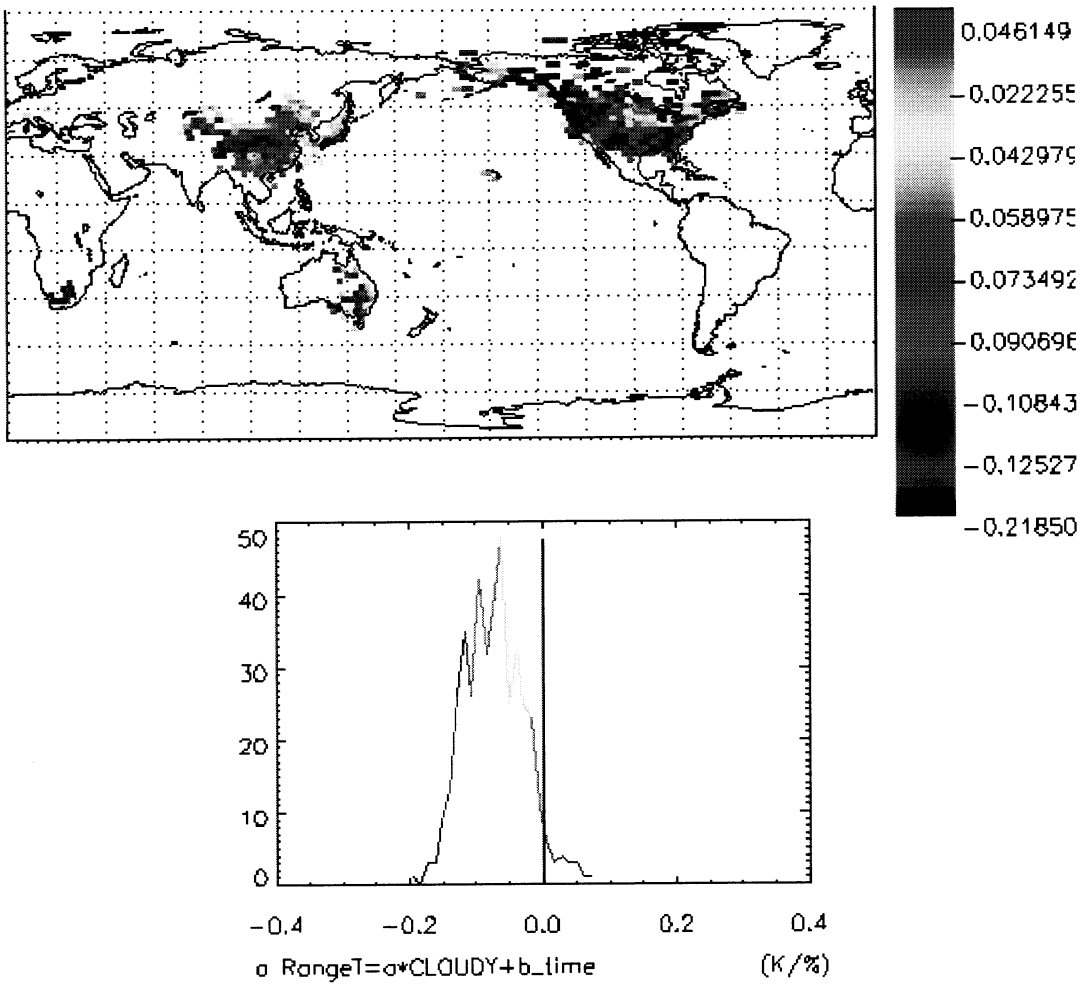

Figure 1. Sensitivity of surface temperature range to cloud fluctuations.

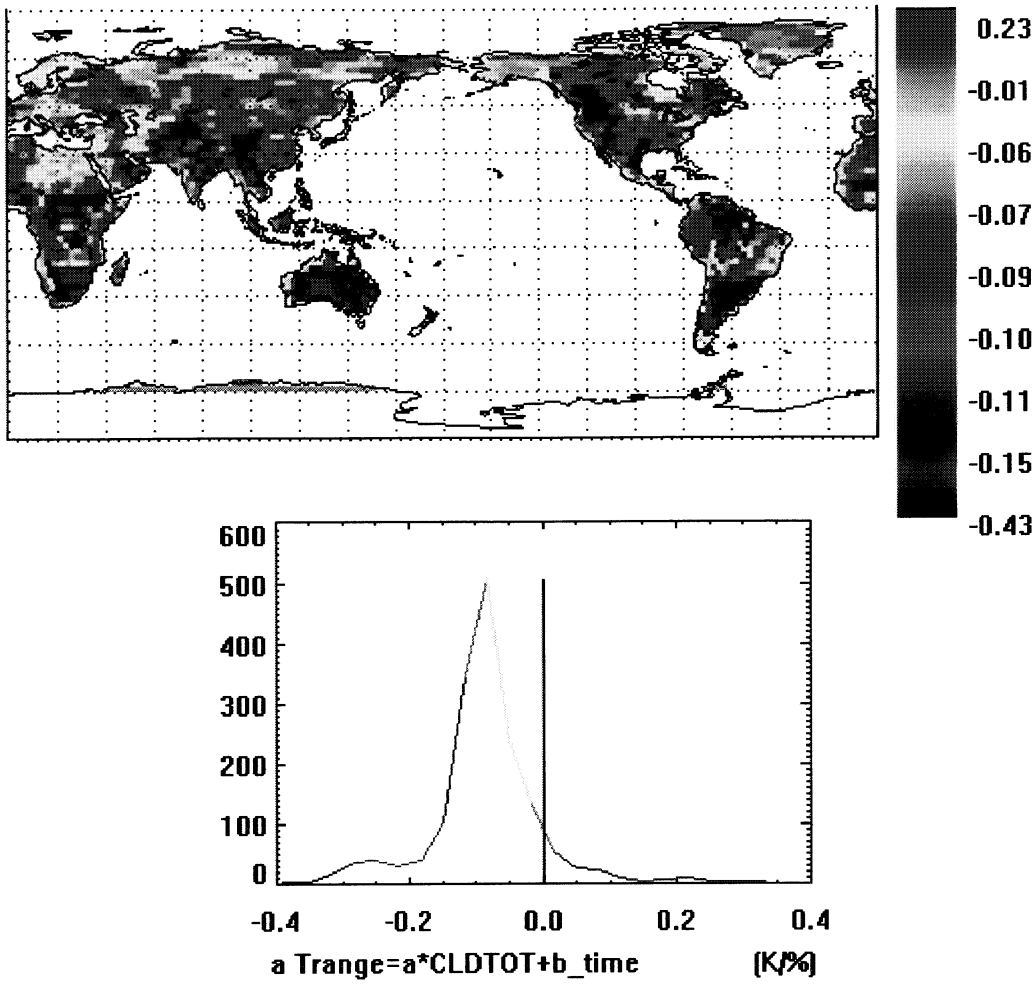

Figure 2. Sensitivity of temperature range to changes in cloudiness.

Wide Field of View Time Series

Over the last 20 years, 5 different satellites have made broad band radiation budget measurements: (see table 1). The Wide Field of View instruments have operated much longer than the scanning instruments and provide the potential to monitor climate fluctuations for 20 years.

Table 1: Wide Field of View Radiation Budget Observations.

Nimbus 6	August 1975	May 1978	Ciesielski et al., 1982
Nimbus 7	November 1978	April 1986	Kyle et al. 1993
ERBE	November 1987	October 1992	Barkstrom, 1984

Some of the ERBE Wide Field of View (WFOV) observations have been reprocessed and extended into the 1990's. Here we used the merged WFOV estimate listed below as the ERBE result. When connected to the Nimbus data, this series will extend for almost 20 years. We constructed a time series of all these data for some empirical studies. Figure 3 shows a time series of Nimbus 6, Nimbus 7 and ERBE Wide Field of View observations. The locations shown in Figures 3 and 4 illustrate some of the difficulties in merging these different data sets. Some of the ERBE months are missing so characterizing the annual cycle has higher error in the ERBE series than the Nimbus 7 series. The ERBE results are the merger of observations at different times and later in the series, from only the ERBS 57° inclined drifting satellite. Because of the local time of measurement and the resulting sun angles, certain months of the ERBS timeseries have large errors as seen in Figure 4 in 1991 and 1992. The amplitude of the Nimbus 6 seasonal cycle is different perhaps because of different analysis schemes.

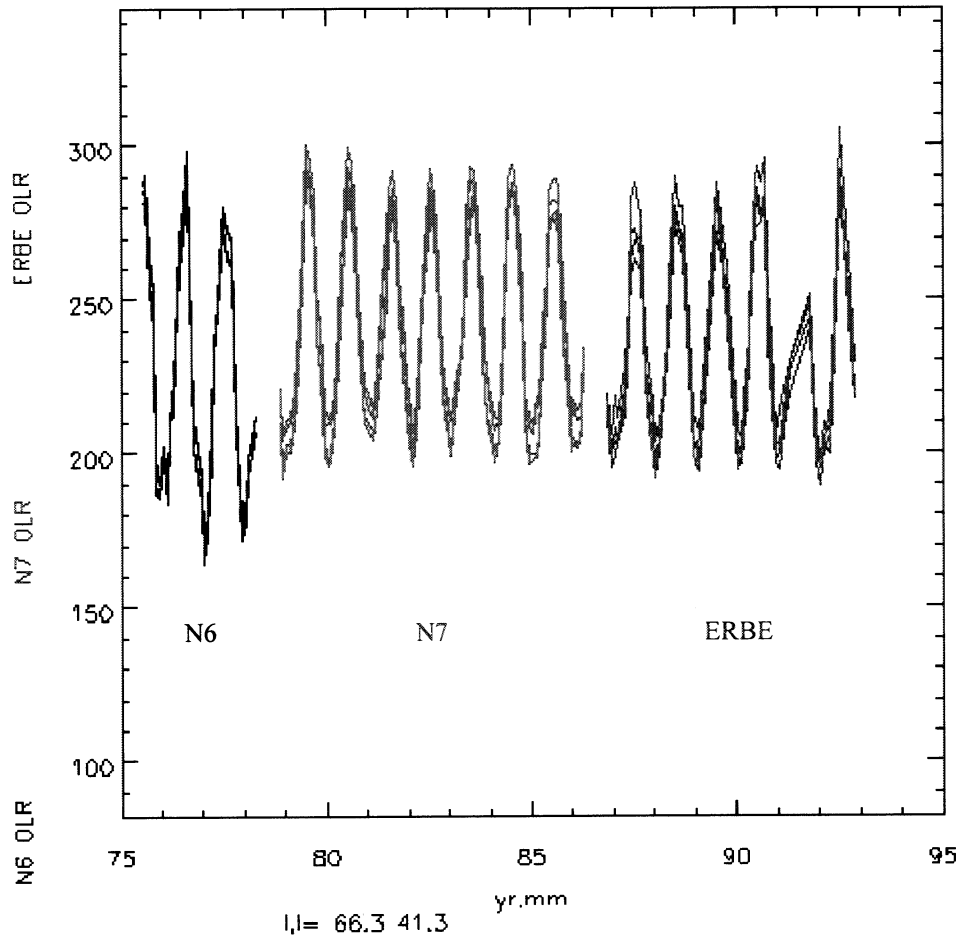

Figure 3: Time series of Wide Field of View observations of outgoing longwave radiation (OLR) above 66° east longitude, 41° north latitude. Four adjacent bins are shown to give some idea of the spatial homogeneity of the observations. Missing months in the ERBE time series are not delineated, but are evident in 1991.

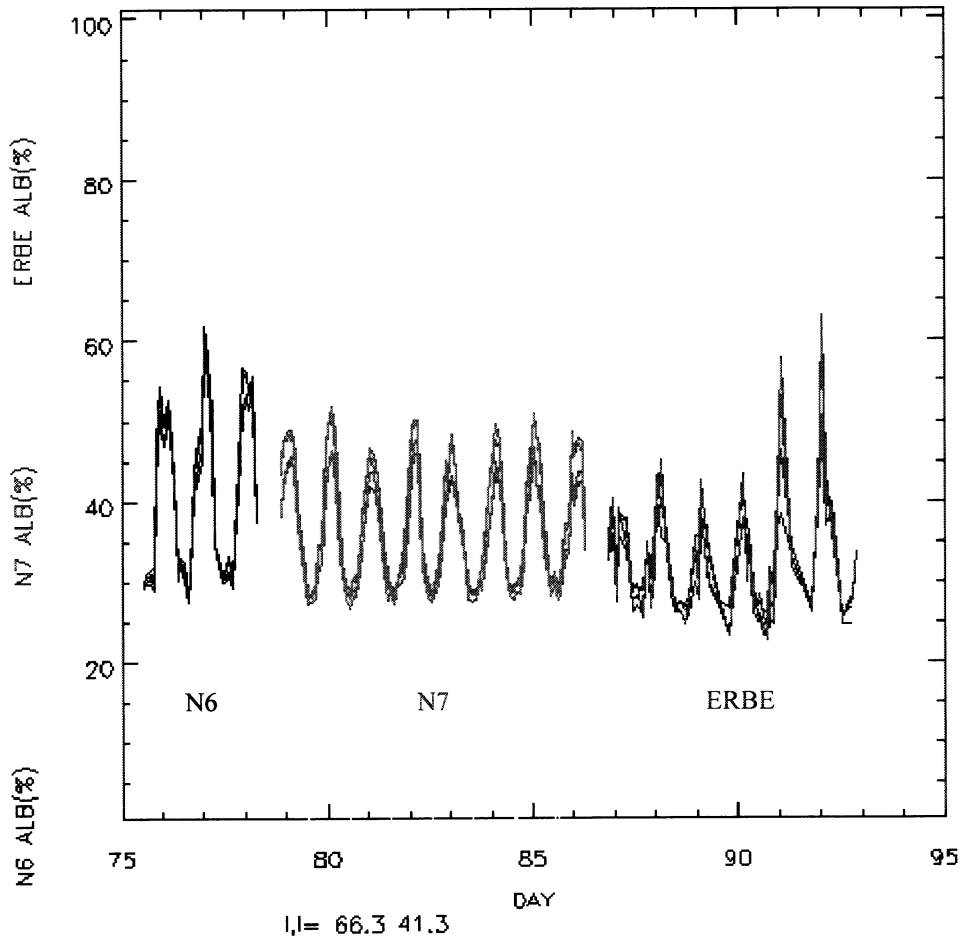

Figure 4: Time series of Wide Field of View observations of albedo above 66 ° east longitude, 41° north latitude. Four adjacent bins are shown to give some idea of the spatial homogeneity of the observations.

It is difficult to merge the data directly into one long time series because of the different girds and because of the different calibration standards. As a first try, we converted each time series into an anomaly series, about the individual series seasonal cycle. We tested fitting the different annual cycles so that one could standardize each satellite to a reference satellite (Figure 5). First zonal means and then multi year averages of each month were constructed for each satellite. Then the Nimbus 6 and ERBE annual cycles at each latitude was regressed against the Nimbus 7 annual cycle. The resulting slope and offsets are shown in Figure 6. The tropical regions between 30 north and 30 south do not have a simple annual cycle so the regression coefficients in those areas were not useful. In the mid-latitudes (north and south) the slopes are significantly different than 1.0. Most important, they are not the same value, so a simple linear regression adjustment to match up the different satellites will not be effective. Some of the very large difference in the tropical areas occurs because the mean weather was different in the different periods. Figure 10 shows the Southern Oscillation Index which is substantially different in the mid 1970's than later years.

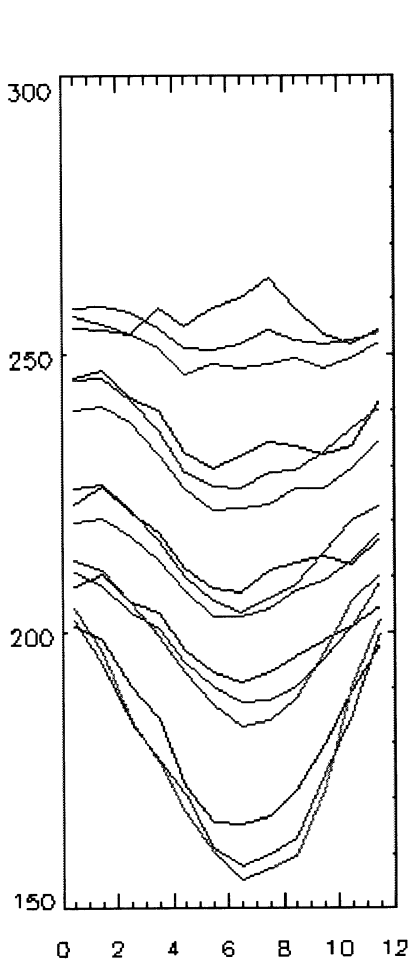

Figure 5. Mean annual cycles for different Southern Hemisphere zones, Nimbus 6 black, Nimbus 7 red and ERBE blue.

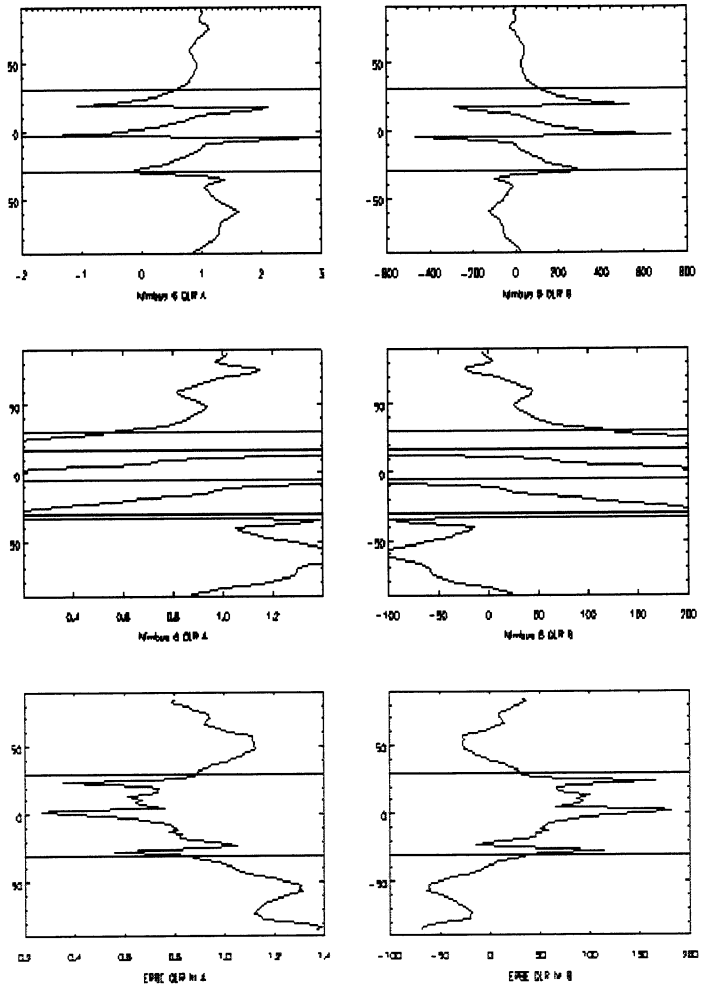

Figure 6, Fits to consider re-calibration of each series to match the Nimbus 7 series.

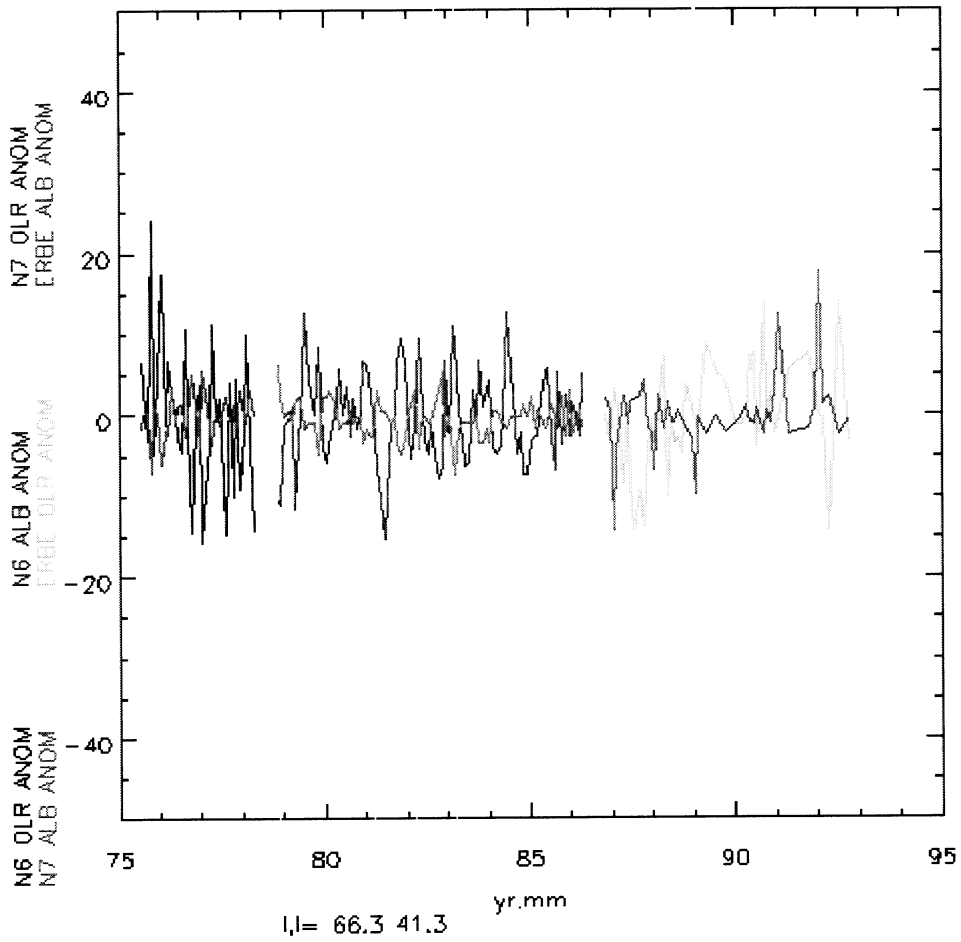

Figure 7: Time series of anomalies above 66 ° east longitude, 41° north latitude. OLR and Albedo anomalies are shown.

Another way to normalize the different data sets is to remove the mean annual cycle measured by each experiment separately. Then the anomaly series might be homogeneous enough to look at year to year fluctuations. Figure 7 shows a plot of the anomalies for the location in Figures 3 and 4. From the variations around the means, this first sight looks like a homogeneous time series. Figure 8 is more interesting because it shows the western Pacific with its obvious El Niño variations. Figure 9 shows this even more strongly. For reference, the Southern Oscillation Index is shown in figure 10. In deed the ERBE fluctuations occur with El Niño events. One should see similar variations in the Nimbus 6 series with the La Niña events of the 1970's. That 2.8-year series is too short to give a climatological annual cycle so the events of those years are not evident.

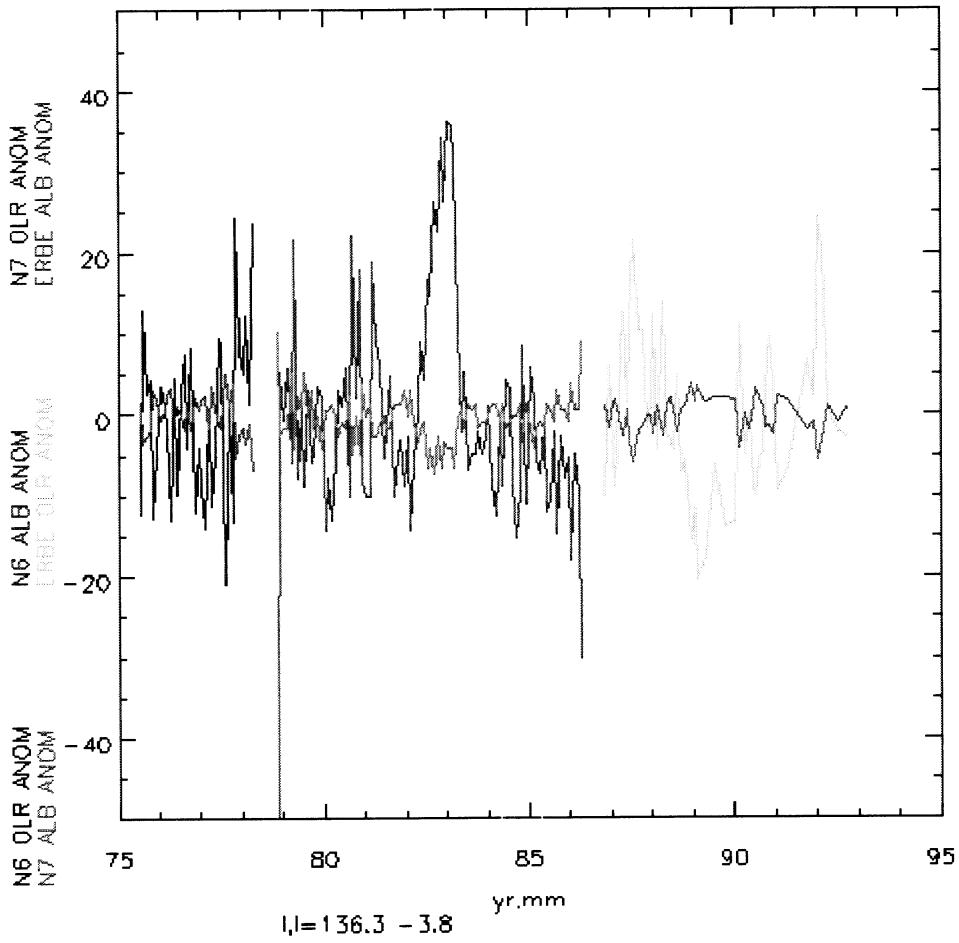

Figure 8. Western Pacific region with the strong El Niño of 1982/83 and the smaller El Niños of the later 80's and 90's. OLR and Albedo anomalies are shown.

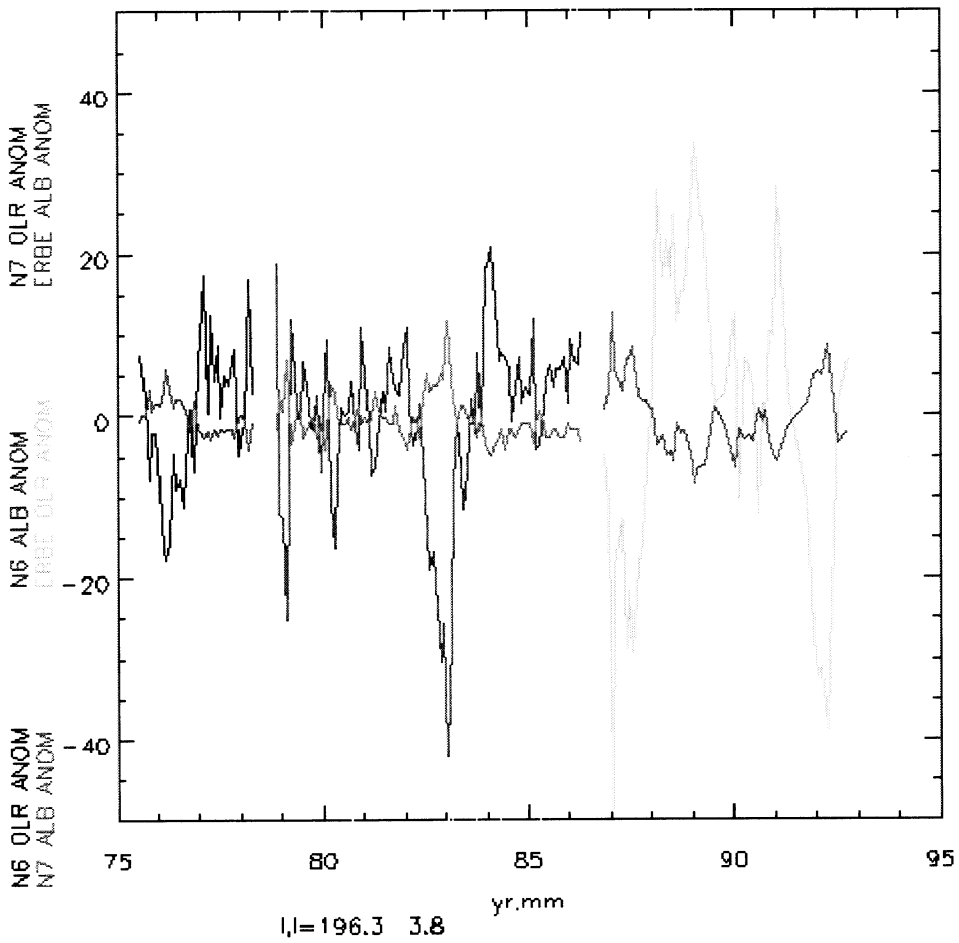

Figure 9. Central Pacific region with El Niño signal. The large fluctuations in the ERBE data occur because of a small shift in the position of the ITCZ in this area. OLR and Albedo anomalies are shown. Clouds produce the ERBE anomalies since both the albedo and the OLR change in a consistent fashion.

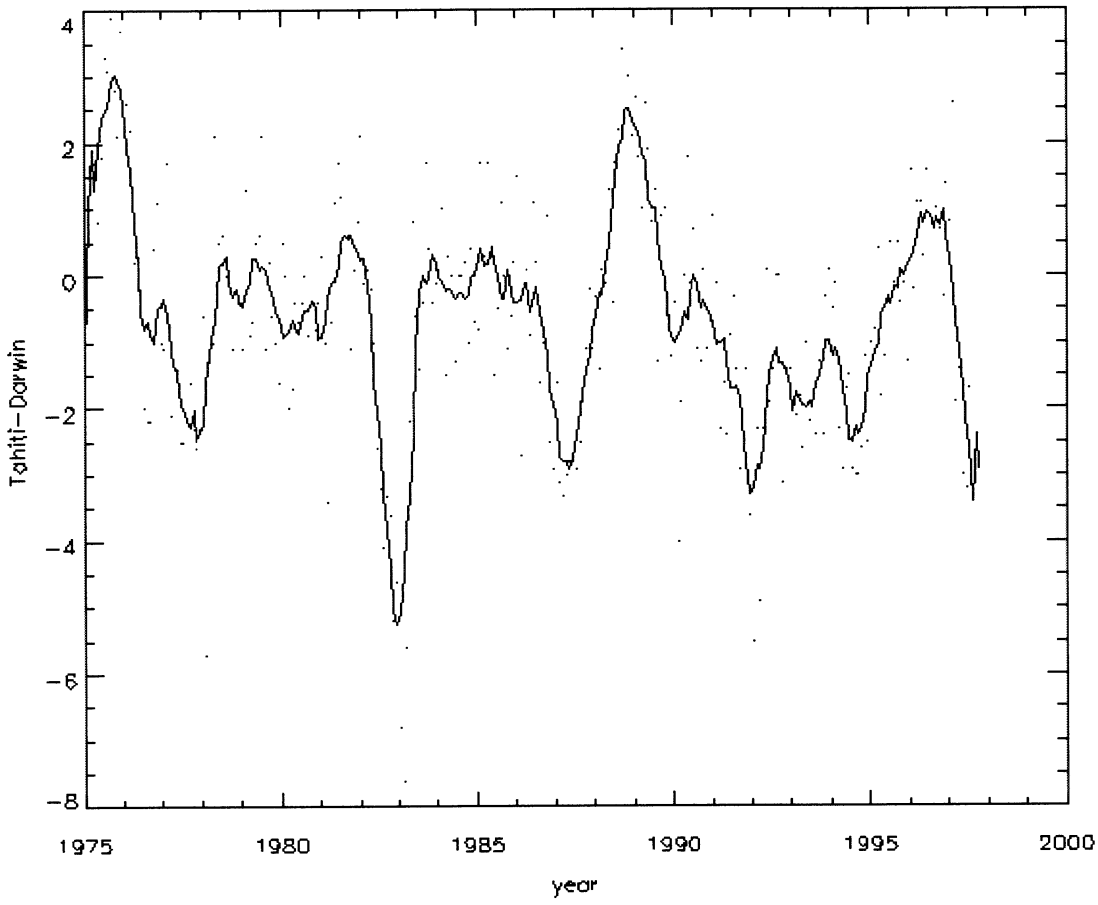

Figure 10. Standardized pressure difference Tahiti minus Darwin smoothed. This provides a first order indication of El Niño / La Niña situations. Data from Nation Climate Data Center.

Another way to look at the results is with large regional averages. Figure shows the globe divided into three regions. Here the missing months in the ERBE series are more obvious.

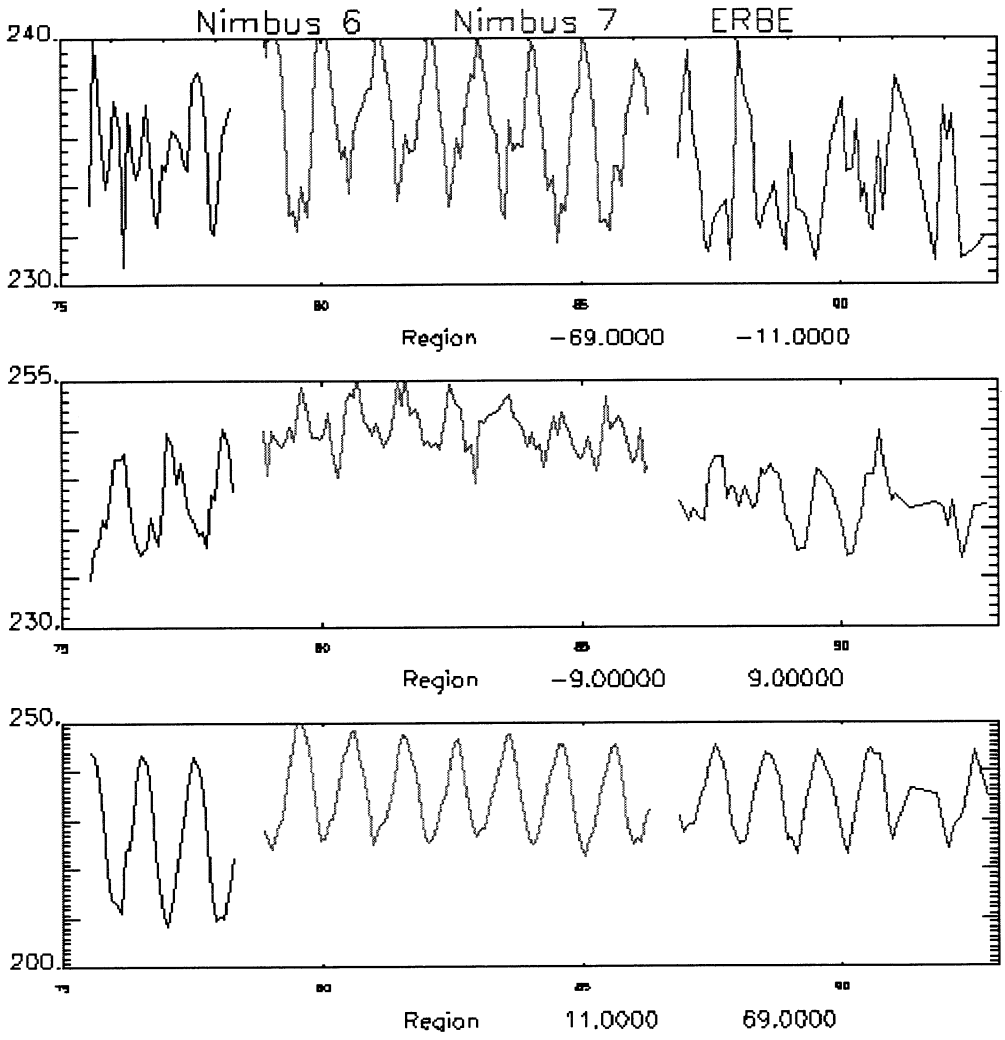

Figure 11. Large regional averages of the OLR data (W/m2). Notice that the range in radiance is smaller for the equatorial and southern regions.

Comparisons between the different measurement systems are not complete because there is considerable data still missing in the reprocessed ERBE time series. Once these additional months are available, we will reconsider this analysis.

We have not attempted to adjust the ERBE or Nimbus data for different diurnal samplings. Different months of ERBE data have different diurnal observation times, which contributes to some of the difference between the observations.

Relationship between water vapor and radiation budget.

In 1995 a comparison was prepared between NVAP data and ERBE. This was included in an earlier report, but is included in Appendix B for completeness.

WWW references.

Some of the information in this report can be seen in more detail on the World Wide Web at the following addresses:

http://www.cira.colostate.edu/Climate/mxmn/mymapmx.HTM Temperature minima and maxima.

http://www.cira.colostate.edu/Climate/wvre/wvre.HTM Water vapor comparison to radiation budget.

http://www.cira.colostate.edu/Climate/NVAP/NVAPCIRA.HTM General water vapor data set description.

Future Research

Merging with other radiation budget data sets is a possibility once the ERBE data reanalysis is completed. A comparison with the NOAA narrow band radiometer Outgoing Longwave Radiation time series is a possibility. The SCARBE and CIRES data sets will become available for the 1990's. Still the lack of overlap between the sensor systems hinders the normalization of the different data sets.

Conclusions

During this research period we have utilized the ERBE data set in comparisons to surface properties and water vapor observations in the atmosphere. The attempt to construct a homogeneous time series from Nimbus 6, Nimbus 7 and ERBE data is not complete because we are still waiting for the ERBE reanalysis to be completed. It will be difficult to merge the Nimbus 6 data in because its observations occurred when the average weather was different than the other periods, so regression adjustments are not effective.

References.

Campbell, G.G. and T.H. Vonder Haar, 1997, 1997: Comparison of Surface Temperature Minimum and Maximum and Satellite Measured Cloudiness and Radiation Budget, *J. Geophy. Res. Atmospheres.*, **102** No. D14, p 16639-16645.

Ciesielski, P.E., T.H. {Vonder Haar}, and G.G. Campbell, 1982, Analysis of Nimbus--6 and Nimbus--7 data as it pertains to the earth radiation budget, Dept. of Atmos. Sci., Colorado State Univ. **364**,Fort Collins, CO.

B.R. Barkstrom, B.R.,1984, The Earth Radiation Budget Experiment (ERBE)}, *BAMS*, **65**, 1170 1185.

Kyle, H.L., J.R. Hickey, P.E. Ardunuy, H. Jacobowitz, A.Arking, G.G. Campbell, F.B.House, R. Maschoff, G.L.Smith, L.L. Stowe, and T.H. Vonder Haar}, 1993, The Nimbus Earth Radiation budget (ERB) Experiment: 1975 to 1992, *BAMS*, 74

Appendix A: Campbell and Vonder Haar paper.

Appendix B: NVAP vs. ERBE from 1995 report.

JOURNAL OF GEOPHYSICAL RESEARCH, VOL. 102, NO. D14, PAGES 16,639–16,645, JULY 27, 1997

Comparison of surface temperature minimum and maximum and satellite measured cloudiness and radiation budget

G. Garrett Campbell and Thomas H. Vonder Haar
Cooperative Institute for Research in the Atmosphere, Colorado State University, Fort Collins

Abstract. Mean surface temperature extremes over land areas during 1983 to 1990 are discussed in terms of satellite-measured cloud and radiation parameters. These show that cloud fluctuations induce changes in the temperatures with the decrease of temperature maximum stronger than the increase of temperature minimum because clouds cause changes in incident shortwave surface flux as well as downward long-wave radiation. Sensitivity to top of the atmosphere radiation is complicated by the intervening clouds and atmosphere. A comparison is also made to a sample general circulation model simulation showing the same effects.

Introduction

The first climate models were energy balance models which parameterized the energy budget in terms of surface temperature [*Simpson*, 1928; *Budyko*, 1969]. Typically these did not parameterize the cloud effects because of their complexity of clouds. More recently, the cloud effects have been discussed in terms of their gross time and space average of the Earth's climate system. The comparison of the mean cloud free situation with the average is termed cloud forcing [*Ramanathan et al.*, 1989; *Vonder Haar*, 1993; *Sohn and Robertson*, 1993). These studies and others demonstrate that the net radiation is decreased by introduction of clouds into the atmosphere. Since different types of clouds have different effects on the surface radiation budget and on the surface temperature [*Stephens and Webster*, 1984], it is not obvious whether clouds cool or warm the surface even if the top of the atmosphere (TOA) radiation budget is decreased.

The relationship between clouds and surface temperature via the surface energy budget is generally weak (as shown below), but there appear to be stronger relationships to temperature extremes over land [*Karl et al.*, 1993]. Discussed below are the sensitivity of the surface temperature extremes to cloud changes and changes in radiation budget. We take the point of view of *Leith* [1973] that climate fluctuations will map out the response of the climate to small changes in forcing functions. *Plantieo et al.*, [1990] have actually detected changes in temperature extremes associated with cloud changes based on surface station measurements over the United States but they do not report the magnitudes of $\Delta T/\Delta$cloud.

The object of this paper is to note and demonstrate that these effects can be directly quantified with satellite-based measurements of clouds or radiation budget. Also shown is that general circulation models (GCMs) can simulate these relationships to some extent, as demonstrated by one example.

G. G. Campbell and T. H. Vonder Haar, CIRA, Colorado State University, Foothills Campus, Fort Collins, CO 80523. (e-mail: campbell@cira.colostate.edu.

Copyright 1997 by the American Geophysical Union.

Paper number 96JD02718.
0148-0227/97/96JD-02718$09.00

Certainly weather will affect any individual day's temperature extremes, and persistent weather features like blocking situations will affect the monthly mean extremes. Here we try to separate out the effects of clouds from other variables. This will be done first by using monthly means which smooth the daily fluctuations and second by removing the seasonal cycle. Finally, the results are based on correlations of these anomalies. The problem of separating cause and effect is a general problem of empirical climate studies, and we rely on the consistency of several parameters besides clouds to support our argument. Comparisons with other parameters like rainfall or other weather regimes would be interesting, but here we focused on the monthly mean cloud effects.

Data

Four sets of observations will be used in this study, as shown in Table 1. The monthly mean minimum and maximum temperatures assembled by *Karl et al.*, [1993] were remapped by area averaging onto an International Satellite Cloud Climatology Project (ISCCP) equal area grid. The ISCCP monthly mean cloud statistics from the C2 data set [*Rossow and Schiffer*, 1991] come from an analysis of data every 3 hours for each day of the month. The surface radiation budget estimate is derived from the ISCCP C1 cloud analysis [*Darnell et al.*, 1992]. The Earth Radiation Budget monthly mean TOA radiation fluxes [*Barkstrom*, 1984] are based on measurements by broadband instruments flown on three satellites.

Empirical Relationships

We assume a physical linkage among the radiation and cloud variables and the surface temperatures via the surface energy budget. We will explore this with statistical regressions.

Time Regression

For the regressions, anomaly series were constructed by subtracting the time average month from each month. For each of the time series a linear regression was used to estimate the relation between temperature (T) and the cloud or radiation parameter (R): $T = s * R + b$. The slope (s) can be interpreted as the sensitivity: $\Delta T/\Delta R$. Figure 1 shows scatterplots and the linear regression line for 90 monthly average anomalies for one sample

Table 1. Data Sets Used

Data Set	Resolution	Time Period
Monthly minimum and maximum temperature surface station observations	remapped to 280 km ISCCP bins Land observations mostly in the Northern Hemisphere midlatitudes.	7/83 to 12/90 (1/60 to 12/90 available)
Monthly ISCCP cloud amount satellite from observations	280 km grid	7/83 to 12/90
Surface radiation budget net, shortwave net, longwave net estimates	280 km grid	7/83 to 12/90
Monthly ERBE TOA flux observations	2.5° grid transformed to the 280 km ISCCP grid	2/85 to 4/89

One certainly would have preferred longer time series of the satellite data, but as will be shown, even with the 90 months of the International Satellite Cloud Climatology Project (ISCCP) or 50 months of the Earth Radiation Budget Experiment (ERBE) significant relationships can be measured between the surface temperatures and the satellite observations and estimates. Top of Atmosphere, TOA.

280 km bin centered at 43°N and 82°W (the Detroit area). The four plots show the relationship between four temperature anomalies: maximum (*T*max); minimum (*T*min); average (*T*max + *T*min)/2; range (*T*max - *T*min) and cloud anomalies. From regressions of all the populated bins a map of the sensitivities can be constructed, as shown in the example in Figure 2. Daily temperature extremes are only of interest over land areas, and reports are only available for limited reporting regions. As shown by the map, this analysis represents about 5% of the globe. For each individual time series, only a modest amount of the variance is explained by the single-parameter fit, reflecting the complex nature of the mean weather.

To summarize the results for all regions, a histogram of the sensitivities show distinct distributions for each of the temperatures studied, as shown in Figure 3. Generally, *T*max is decreased when cloud amount is higher than normal. Similarly, *T*min increases with more clouds. There are many regions which show opposite effects, but these are the predominant effect because of the noise of other sources of variability. For almost all locations the range is decreased by increasing clouds. In contrast, the sensitivities to the average overlaps zero. This demonstrates that the mean temperature is relatively insensitive to external perturbations.

Space Regression

Another approach for estimating $\Delta T/\Delta R$ is to take all the observations distributed across a region or the globe for the fit.

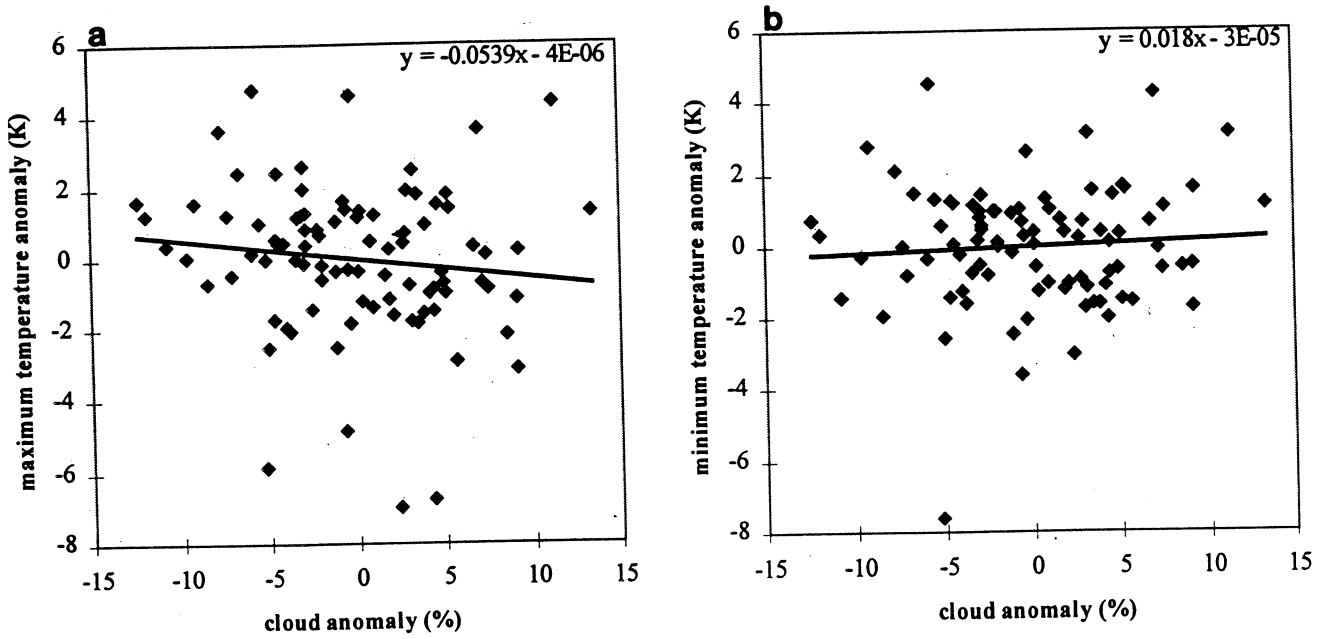

Figure 1. Scatterplots of the temperature anomalies and cloud amount anomalies. Each point represents 1 month International Satellite Cloud Climatology Project 280 km bin centered at 43°N and 82°W between 1983 and 1990. The $\Delta T/\Delta$cloud sensitivities are estimated from the linear regression slopes.

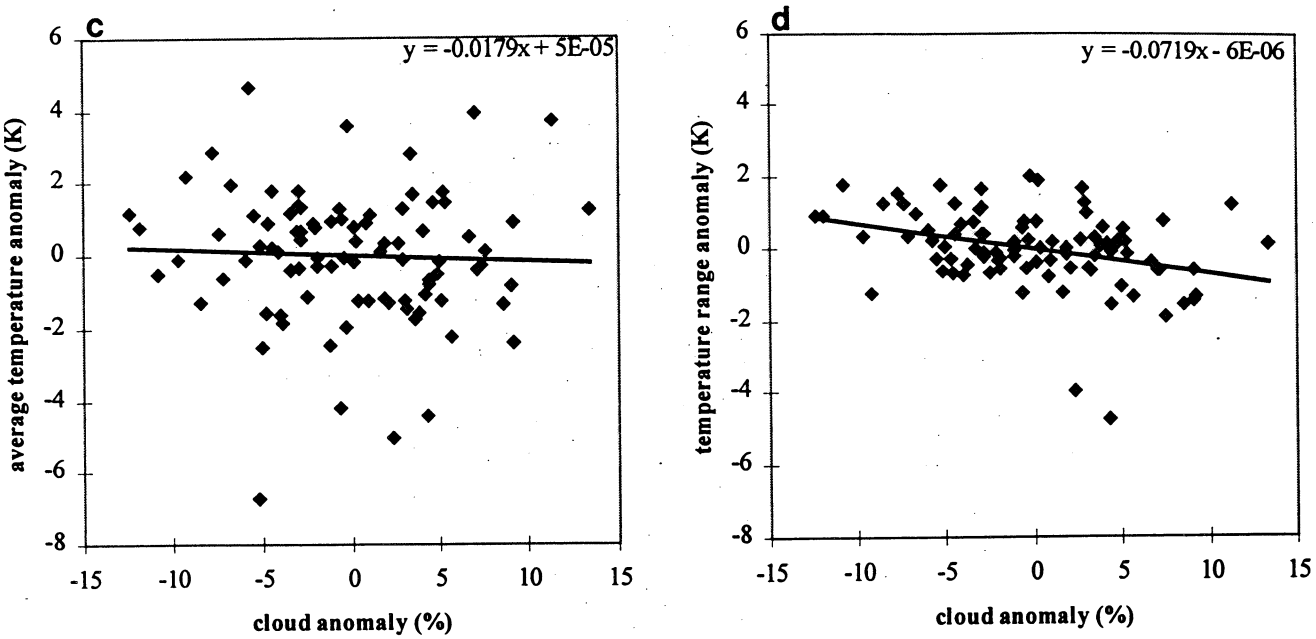

Figure 1. (continued)

One ends up with a regression for each time. This was used because of the shortness of the ERBE time series. Figure 4 shows series of slopes and the corresponding histogram of sensitivities. The distinct positions of the histograms in the time as well as space fits has lead us to the following analysis.

Results

One may hypothesize that the maximum surface temperature will be decreased when there are more clouds [*Stephens and Webster*, 1984]. This would occur because there would be less downward solar radiation during the daytime when the maximum would most likely occur. For the minimum temperature the clouds would act to raise the minimum because more clouds will produce larger downward infrared (IR) flux. Alternately, temperature anomalies could cause cloud changes or the associations are random.

To summarize the results, the averages of the sensitivities and the width of the frequency distribution (i.e., Figure 3) as estimated by the standard deviation of the means are shown in Tables 2 and 3. Although the distributions are not Gaussian, the standard deviation of the mean is some measure of the width of the histogram and the uncertainty of the mean. As seen in the tables, most of the differences of the means are larger than the uncertainty, so the results are statistically significant. Ultimately, we are comparing different frequency distributions to see if they are distinct. The standard deviation of the mean is a measure of the uncertainty of the mean. Perhaps more convincing is the fact that the two analysis methods generally agree. Most of the parameters show results consistent with the hypothesis that

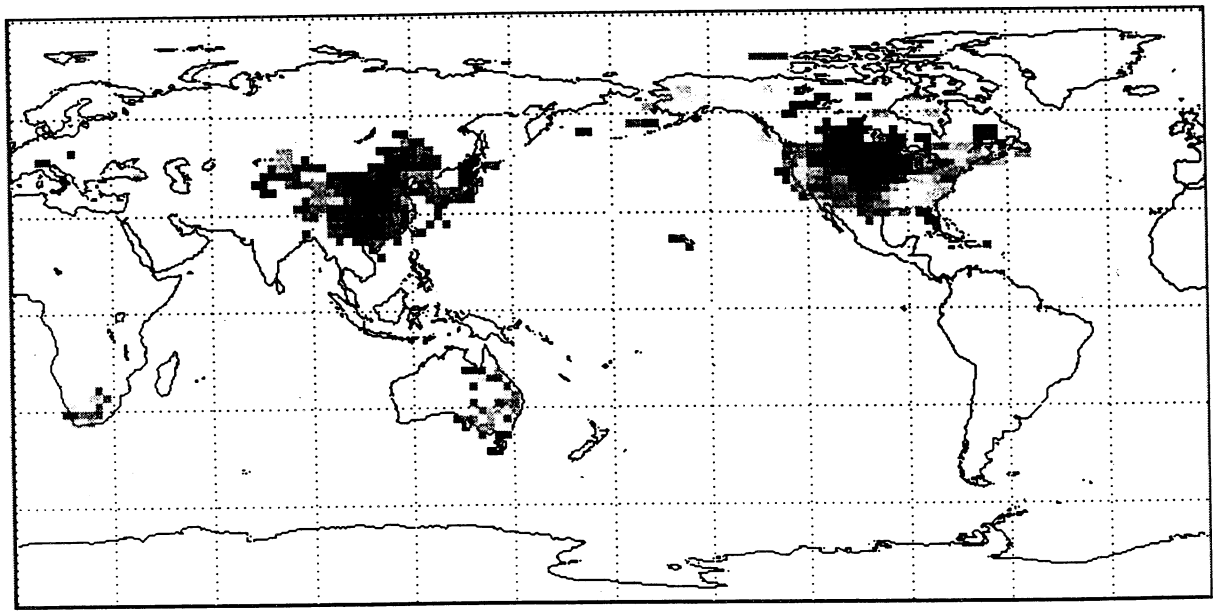

Figure 2. Map of sensitivities of $\Delta T\text{max}/\Delta\text{cloud}$. This shows some geographic consistency in the sensitivity and the limited geographic region sampled by the *T*min/*T*max data set.

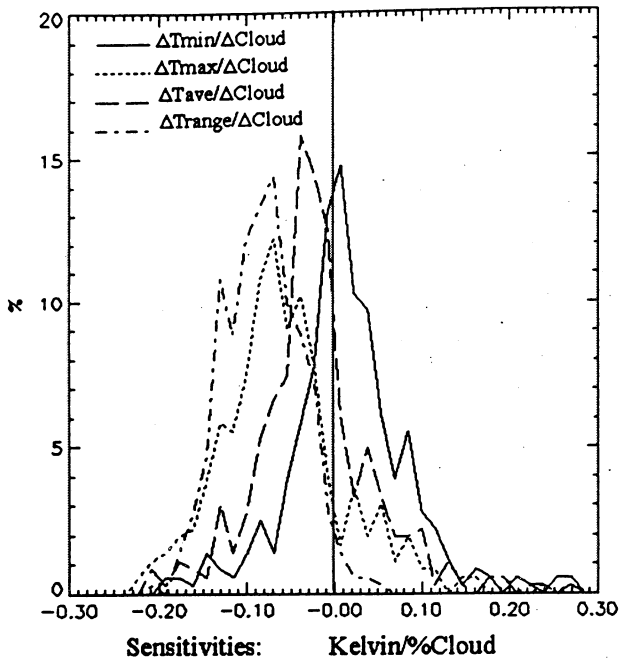

Figure 3. Histogram of ΔTmin/Δcloud, ΔTmax/Δcloud, Δ(Tmin+Tmax)/2/Δcloud, and ΔTrange/Δcloud from time fits. These show the frequency of occurrence of different sensitivity values for all the occupied bins distributed like the map in Figure 2.

clouds have a strong influence on the ground temperatures via the surface radiation effects.

As shown by the tables, clouds or radiation terms explain only a small amount of the variances of the temperature anomalies. In contrast, regressions between cloud and TOA flux show that clouds can explain a very substantial amount of the variance. Calculating with the analysis methods used for temperature anomalies, more than 25% of the variance of the longwave or shortwave fluxes is explained by the ISCCP cloud amount fluctuations over the whole globe or just in the northern midlatitudes.

Discussion

Referring to the tables, some consistency is seen between the results which might be summarized as ΔTmin/Δcloud ~ 0.026 K/% and ΔTmax/Δcloud ~ -0.049 K/%. This is consistent with the blanketing effect of cloud at the surface, as seen in the sensitivity to surface radiation budget (SRB), the true forcing of the surface temperature. The opposite effects of the two processes lead to a much smaller effect on the average of the temperature extremes, as mentioned in the introduction. Since both terms supplement each other in the range calculation, the sensitivity to the daily range is stronger with more clouds decreasing the difference in the extremes. Generally, the explained variance of the temperature range is much bigger than the other $\Delta T/\Delta R$, so it provides a more robust signal for model comparison or detection of regional climate or mean weather changes.

To make an easier scan of the tables, a bold circle has been placed next to the sensitivities which are consistent with the idea that clouds warm the minimum by increasing the downward IR flux and cool the maximum because the decreased shortwave radiation is larger than the increased downward IR. A question mark shows contradictory results.

The analysis of the particular ISCCP cloud types shows that only a small amount of the variance of the temperatures can be explained by each type. The low cloud sensitivity disagrees with our hypothesis, perhaps because anomalies in these clouds are associated with cold events. Middle and high clouds agree somewhat better with the hypothesis with ΔTmin/Δhigh cloud showing a net warming effect showing that the change in

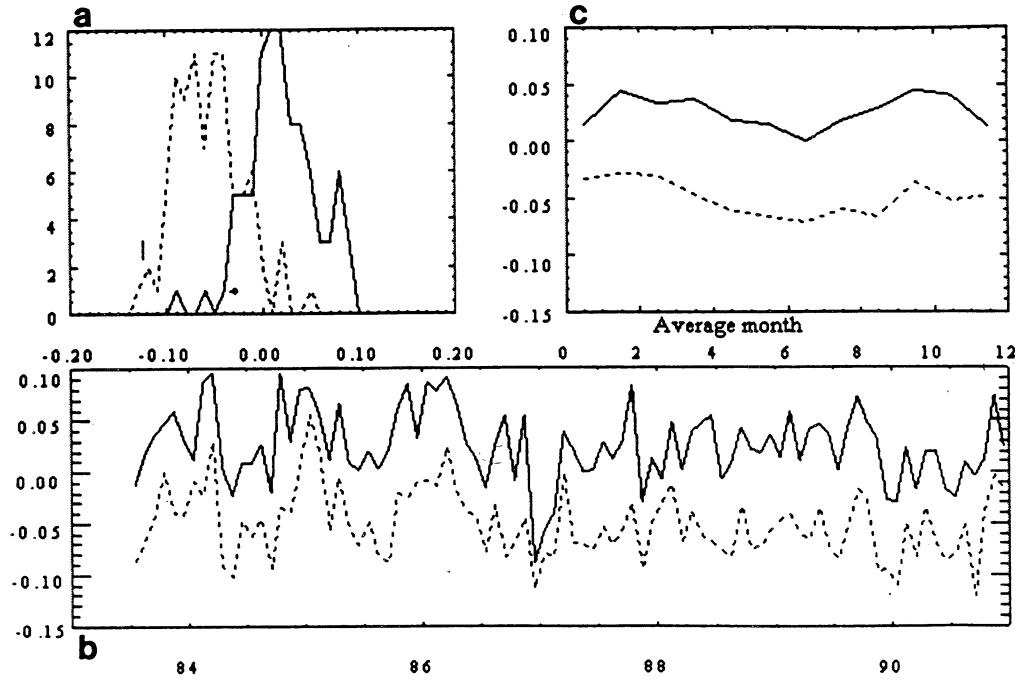

Figure 4. (a) Histogram of ΔTmin/Δcloud from space fits. ΔTmax/Δcloud dotted. ΔTmin/Δcloud solid; (b) Time series of ΔT/min/Δcloud from space fits for all populated bins (5% of globe); (c) Seasonal composite of the series in Figure 4a showing that there is only a moderate seasonal cycle.

Table 2. Sensitivities Derived From Space Fits

Space Fit Observed, $\Delta T/\Delta R$	ΔTmin, K			ΔTmax, K			$\Delta(T\text{min}+T\text{max})/2$, K			$\Delta(T\text{max}-T\text{min})$, K		
ΔCloud, %	0.0254	0.0038 ●	6%	-0.0503	0.0036 ●	9%	-0.0125	0.0034 ●	4%	-0.0757	0.0026 ●	20%
ΔLow cloud, %	-0.0530	0.0080 ?	3%	-0.0355	0.0081 ●	2%	-0.0443	0.0078	3%	0.0175	0.0040	2%
ΔMid cloud, %	0.0014	0.0067	3%	-0.0902	0.0068 ●	8%	-0.0444	0.0062	5%	-0.0915	0.0053 ●	9%
ΔHigh cloud, %	0.0635	0.0067 ●	7%	-0.0238	0.0066 ●	5%	0.0199	0.0064	4%	-0.0872	0.0036 ●	13%
ΔSRB Net, W/m²	-0.0109	0.0025	2%	0.0211	0.0028	5%	0.0051	0.0025	3%	0.0321	0.0019	7%
ΔSRB Net Down, (LW+SW), W/m²	0.0226	0.0032 ●	7%	0.0568	0.0029 ●	25%	0.0397	0.0030 ●	17%	0.0341	0.0015 ●	18%
ΔSRB LW Down, W/m²	0.0735	0.0044 ●	24%	0.0743	0.0040 ●	18%	0.0739	0.0040 ●	25%	0.0008	0.0022 ●	2%
ΔSRB SW Net, W/m²	-0.0134	0.0023	4%	0.0364	0.0021 ●	12%	0.0115	0.0020	5%	0.0499	0.0020 ●	22%
ΔERBE TOA LW Absorbed, W/m²	-0.0086	0.0064	4%	-0.0899	0.0051 ?	14%	-0.0492	0.0055 ?	7%	-0.0813	0.0037 ?	19%
ΔERBE TOA SW Absorbed, W/m²	-0.0031	0.0037	4%	0.0515	0.0033 ●	12%	-0.0242	0.0030	6%	0.0546	0.0035 ●	20%
ΔERBE TOA Net, W/m²	-0.0185	0.0055	4%	0.0290	0.0053 ●	7%	0.0053	0.0050	4%	0.0475	0.0040 ●	13%

Each box lists three numbers: the mean $\Delta T/\Delta R$, standard deviation of the mean, and the average explained variance for the many fits included in the mean. The bold circle or question mark indicate agreement or disagreement with the simple hypothesis discussed in the text. LW, longwave; SW, shortwave; SRB, Surface Radiation Budget.

Table 3. Sensitivities Derived From Time Fits Like Table 2

Time Fit Observed, $\Delta T/\Delta R$	ΔTmin, K			ΔTmax, K			$\Delta(T\text{min}+T\text{max})/2$, K			$\Delta(T\text{max}-T\text{min})$, K		
ΔCloud, %	0.0265	0.0035 ●	8%	-0.0477	0.0035 ●	11%	-0.0106	0.0033 ●	6%	-0.0741	0.0021 ●	26%
ΔLow cloud, %	-0.0523	0.0054	4%	-0.0210	0.0062	4%	-0.0367	0.0054	4%	0.0313	0.0046	4%
ΔMidcloud, %	0.0037	0.0056	6%	-0.0962	0.0057	9%	-0.0462	0.0053	6%	-0.0998	0.0040	4%
ΔHigh cloud, %	0.0839	0.0046 ●	9%	-0.0031	0.0050 ●	7%	0.0404	0.0045	5%	-0.0870	0.0034 ●	17%
ΔSRB net, W/m²	-0.0064	0.0014	3%	0.0237	0.0017	6%	0.0086	0.0014	4%	0.0301	0.0015	11%
ΔSRB net down (LW+SW), W/m²	0.0248	0.0013 ●	8%	0.0576	0.0015 ●	27%	0.0412	0.0013 ●	18%	0.0327	0.0010 ●	22%
ΔSRB LW down, W/m²	0.0816	0.0024 ●	27%	0.0824	0.0027 ●	24%	0.0820	0.0024 ●	28%	0.0007	0.0014 ●	4%
ΔSRB SW net, W/m²	-0.0084	0.0015	4%	0.0387	0.0018 ●	14%	0.0151	0.0015	6%	0.0471	0.0013 ●	29%
ΔERBE TOA LW absorbed, W/m²	-0.0339	0.0046	8%	-0.1102	0.0043 ?	21%	-0.0721	0.0043 ?	14%	-0.0763	0.0025 ?	25%
ΔERBE TOA SW absorbed, W/m²	0.0015	0.0015	4%	0.0364	0.0017 ●	12%	0.0190	0.0015	7%	0.0348	0.0013 ●	18%
ΔERBE TOA net, W/m²	-0.0141	0.0036	7%	0.0308	0.0042 ●	10%	0.0084	0.0037	7%	0.0449	0.0025 ●	16%

Table 4. Sensitivities Derived From Time Fits for CCM 5 Year Simulation

Time Fit CCM, $\Delta T/\Delta R$	ΔTmin, K			ΔTmax, K			$\Delta(T$min+Tmax)/2, K			$\Delta(T$max-Tmin), K		
ΔCloud, %	0.0541	0.0019	16%	-0.0367	0.0022	9%	0.0087	0.0019	6%	-0.0908	0.0012	45%
ΔNet LW surface, W/m²	-0.0305	0.0022	13%	0.0685	0.0021	19%	0.0190	0.0021	8%	0.0990	0.0011	59%
ΔNet SW surface, W/m²	-0.0338	0.0035	11%	0.0675	0.0028	17%	0.0169	0.0029	8%	0.1013	0.0024	42%
ΔTOA LW net, W/m²	0.0081	0.0030	9%	0.0944	0.0030	22%	0.0512	0.0029	11%	0.0863	0.0013	40%
ΔTOA SW net, W/m²	-0.0038	0.0032	8%	0.0954	0.0027	21%	0.0458	0.0027	10%	0.0992	0.0025	37%

Sixty months contributed to the time series analysis at each location. Land areas from 20° to 50°N were used to be similar to the observational data set. Each box lists three numbers: the mean $\Delta T/\Delta R$, standard deviation of the mean, and the average percent explained variance for the many fits included in the mean.

Table 5. Sensitivities Derived From Time Fits for CCM 5 Year Simulation

Space Fit CCM, $\Delta T/\Delta R$	ΔTmin, K			ΔTmax, K			$\Delta(T$min+Tmax)/2, K			$\Delta(T$max-Tmin), K		
ΔCloud, %	0.0511	0.0045	0%	-0.0407	0.0045	8%	0.0052	0.0044	4%	-0.0918	0.0017	43%
ΔNet LW surface, W/m²	-0.0305	0.0040	6%	0.0697	0.0039	19%	0.0196	0.0038	6%	0.1003	0.0016	60%
ΔNet SW surface, W/m²	-0.0111	0.0037	2%	0.0704	0.0034	15%	0.0296	0.0031	6%	0.0815	0.0034	34%
ΔTOA LW net, W/m²	-0.0089	0.0038	3%	0.0736	0.0040	19%	0.0324	0.0038	8%	0.0826	0.0017	39%
ΔTOA SW net, W/m²	0.0050	0.0039	2%	0.0862	0.0037	17%	0.0456	0.0033	8%	0.0812	0.0037	28%

Sixty months contributed to the time series analysis at each location. Land areas from 20° to 50°N were used to be similar to the observational data set. Each box lists three numbers: the mean $\Delta T/\Delta R$, standard deviation of the mean, and the average percent explained variance for the many fits included in the mean.

downward IR is effective at night, and the IR and shortwave effects are about balanced in the daytime. Each of different cloud types appears to decrease the temperature range. We looked at the surface radiation estimates to look for these effects.

The ISCCP data can be separated into clouds at different local times (8/day). Very similar correlations were found comparing morning clouds to Tmin and afternoon clouds to Tmax. Since the surface radiation terms could not be separated into local times, these results were not presented in this paper.

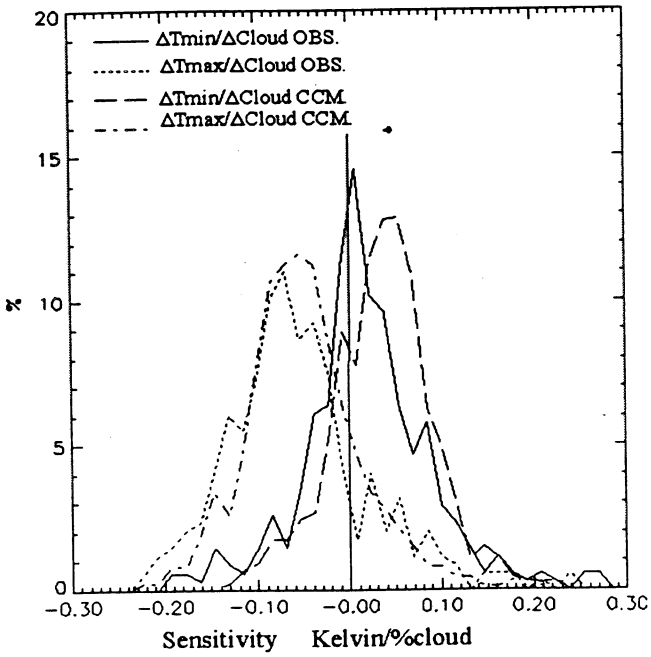

The low and middle cloud amounts are subject to obscuration by the higher clouds because of the satellite point of view. Overlap adjustments are made in the surface radiation budget estimation [*Darnell et al.*, 1992], but we chose to use the direct observations with the idea that fluctuations between months would be similar with or without overlap adjustments.

The surface flux-sensitivities from the table show that downward longwave radiation warms the surface temperature either in the minimum or in the maximum, $\Delta T/\Delta$LW ~ 0.08 K/(W/m^2). As might be expected, the Tmin is not strongly effected by changes in the shortwave surface flux since the Tmin usually occurs during the night. The estimate of ΔTmax/ΔSW shows warming of Tmax, but this is complicated by the fact that fluctuations of shortwave flux are negatively correlated with longwave flux. Just using the observations, we can not hold all but one variable constant to estimate true partial derivatives, so mixtures of effects complicates the analysis. Combining the long and shortwave down terms, there is more sensitivity of Tmax than Tmin to additional downward radiation.

The connections to fluctuations in TOA radiation are less direct being especially complicated for multilayer clouds. The sensitivities to longwave radiation at first sight seems contradictory. More absorbed longwave or less emission to space seems to decrease Tmax. This is caused by the fact that less emission is associated with clouds which are actually producing more downward longwave radiation. Again this arises

Figure 5. Comparison with the National Center for Atmospheric Research community climate model (CCM) result: histogram of ΔTmin/Δcloud, ΔTmin/Δcloud from observations and the same pair of parameters from the CCM analysis for the land areas between 20° and 50°N.

because there is no way to estimate true partial derivatives. The sensitivity to TOA shortwave radiation is closely related to the surface temperature response because most of the shortwave radiation is absorbed by the surface.

The comparisons to the TOA radiation budget correspond to studies of energy balance models [*North*, 1975; *Warren and Schneider*, 1979; *Kiehl*, 1995]. For these simple models, attempts were made to summarize the energy budget in terms of a temperature parameterization: flux = c T + d. Using annual average and seasonal fluctuations, *Warren and Schneider* [1979] estimated c to be 1.6 W/m^2/K for TOA longwave flux. The numbers in Tables 2 and 3 correspond to the reciprocal of c (1/c = 0.625 K/(W/m^2). Our empirical sensitivity observations are much smaller than the energy balance estimates. This implies that the surface temperature is much more difficult to change than these simple energy balance models simulate.

Comparison with Typical GCM Simulation

To put these results in context, a very similar analysis was conducted with a climatological simulation by the National Center for Atmospheric Research (NCAR) community climate model (CCM) [*Bonan*, 1994]. Five years of monthly mean cloud amounts and radiation budgets were compared to monthly temperature extremes. This particular example was selected from the public domain CCM2 histories made available by NCAR. Certainly, longer special runs of the GCM with diurnal cycles are possible but executing a special run was beyond the scope of this study. The particular 5 years used are the last five years of a 10 year simulation which has not come completely to equilibrium [*G.B. Bonan*, personal communication, 1995]. It included a diurnal cycle and a detailed surface parameterization, BATS [*Dickinson et al.*, 1993], but not an interactive ocean. This was appropriate for this comparison because Tmin and Tmax variation over the ocean involves different physics, and our observational study did not include ocean areas. Tables 4 and 5 show sensitivities similar to Tables 2 and 3. The model history did not include identical parameters, especially in terms of the cloud amounts, so comparison to separate cloud layers was not attempted.

The simulation shows that clouds warm the minimum and cool the maximum temperatures. Figure 5 shows a comparison of frequency distributions of sensitivities for the same regions showing the distinct histograms and similarity of the CCM and real world. The numerical values of ΔTmin/Δcloud ~ 0.052 K/% and ΔTmax/Δcloud ~ -0.038 K/% are different than the observational estimate but close enough to give confidence that the model and the real world behave in a somewhat similar way. Noteworthy is the fact that more of the variance of the temperature range is explained by the cloud and radiation fluctuations in the model than the observations.

By treating the GCM as if it were data, the effective sensitivity of the surface parameterization and the model radiation modules is being estimated. Because the area covered by the observations is limited, we do not think that precise numerical matches are required between the simulation and the observation. We are investigating some of the Atmospheric Model Intercomparison Project [*Cess et al.*, 1993] simulations which match the times of the observational record as appropriate for more precise matching. This might lead to a constraint on the simulation which would lead to better parameterization. The sensitivity of Tmin to clouds was stronger in the model, perhaps indicating that this simulation scheme needs some adjustment to the nighttime cloud prediction scheme.

Conclusions

Clouds have a much stronger effect on the range of diurnal temperature change than their effect on the mean. This matches the measured response in sensitivity to changes in surface radiation budget. One is reminded that changes in the near-surface climate, where we live, are more important than TOA radiation budget.

The linear regressions do not explain a large fraction of the variance of the temperature. This implies that the clouds and radiation affect the temperatures, but they are no means the sole control of the temperature. However, the consistency of the relationships with the qualitative theory provides confidence in the idea that clouds moderate the surface climate. The small absolute values of the sensitivities [$\Delta T/\Delta R$] imply that climate is insensitive to cloud fluctuations.

Acknowledgments. This research was supported under the NASA ERBE-2 project (contract NAGW-4122) and NOAA with their support of ISCCP project (contract NA37-RJ0202). The authors wish to specially thank Thomas Karl and his associates for making the temperature data easily available. Thanks also to Nancy Ritchey for making the surface radiation budget available. We thank David Randel for critical discussion and Tony Smith for editorial review.

References

Barkstrom, B.R., The Earth Radiation Budget Experiment (ERBE), *Bull. Am. Meteorol. Soc., 65*, 1170-1185, 1984.

Bonan, G.B., Comparisons of the land surface climatology of the National Center for Atmospheric Research community climate model 2 at R15 and T42 resolutions with implications for subgrid land surface heterogeneity, *J. Geophys. Res., 99*, 10,357-10,364, 1994.

Budyko, M.I., The effect of solar radiation variations on the climate of the earth, *Tellus, 14*, 102-115, 1969.

Darnell, W. L., W. F. Staylor, S. K. Gupta, N. A. Ritchey, and A. C. Wilber, Seasonal variation of surface radiation budget derived from International Satellite Cloud Climatology Project C1 data, *J. Geophys. Res., 97*, 15,741 - 15,760, 1992.

Dickinson, R.E., A. Henderson-Sellers, and P. Kennedy, Biosphere-atmosphere transfer scheme (BATS) version 1 coupled to the NCAR community climate model, *NCAR Tech.* Note, TN-*387*, Nat. Cent. for Atmos. Res. Boulder, Colo., 1993.

Karl, T.R., P.D. Jones, R.W. Knight, G. Kukla, N. Plummer, V. Razuvayev, K.P. Gallo, J. Lindseay, R.J. Carlson, and T.C. Peterson, Asymmetric trends of daily maximum and minimum temperature, *Bull. Am. Meteorol. Soc., 74*, 1007-1022, 1993.

Kiehl, J.T., Atmospheric circulation models in *Climate System Modeling*, edited by K. Trenbreth, Cambridge Univ. Press, New York, 1995.

Leith, C.E., The standard error of time average estimates of climatic means, *J. Appl. Meteorol., 12*, 1066-1069, 1973.

North, G.R., Theory of energy-balance climate models, *J. Atmos. Sci., 32*, 2033-2043, 1975.

Plantico, M.S., T.R. Karl, G. Kukla and J. Gavin, Is recent climate change across the United States related to rising levels of anthropogenic greenhouse gases?, *J. Geophys. Res., 95*, 16,617-16,637, 1990

Ramanathan, V., R.D. Cess, E.F. Harrison, P. Minnis, B.R. Barkstrom, E. Ahmad, and D. Hartman, Cloud-radiative forcing and climate: Results from the Earth Radiation Budget Experiment, *Science, 243*, 57-63, 1989.

Rossow, W.B., and R.A. Schiffer, ISCCP cloud data products, *Bull. Am. Meteorol. Soc., 72*, 2-20, 1991.

Simpson, G.C., Further studies in terrestrial radiation, *Mem. R. Meteorol. Soc.*, III, 1-26, 1928.

Sohn, B.J., and F.R. Robertson, Intercomparison of observed cloud radiative forcing: A zonal and global perspective, *Bull. Am. Meteorol. Soc., 74*, 997-1006, 1993.

Stephens, G.L., and P.J. Webster, Clouds and climate: Sensitivity of simple systems, *J. Atmos. Sci., 38*, 235-247, 1984.

Vonder Haar, T.H., The global energy budget and satellite observations, *Adv. Space Res., 14*(1), 1131-1144, 1994.

Warren, S.G., and S. H. Schneider, Seasonal simulation as a test for uncertainties in the parameterizations of a Budyko-Sellers zonal climate model, *J. Atmos. Sci., 36*, 1377-1391, 1979.

(Received January 29, 1996; revised August 21, 1996;
accepted August 21, 1996.)

Appendix B

The Observed Radiative Effect of Water Vapor and its Variability: A Study Using the ERBE and NVAP Datasets

David L. Randel, Thomas H. Vonder Haar, G. Garrett Campbell
Cooperative Institute for Research in the Atmosphere
Colorado State University

NASA Project NAGW-4122

Presented at the ERBE Science Team Meeting
SUNY Stony Brook
April 3,1995

In this study the radiative effect of water vapor is examined. Our technique develops a statistically significant regression relationship between the clear-sky outgoing longwave radiation (OLR) and the total integrated precipitable water (PWC). Since water vapor absorbs OLR, increases in total column water vapor (WV) should be reflected in decreased OLR and vice-versa.

We used the daily gridded clear-sky OLR from the ERBS and NOAA-10 combination. Daily fields of CS-OLR were examined for the entire year of 1988. For the integrated water vapor we used a dataset from the NASA Water Vapor Project (NVAP) - a daily 1x1 degree global analysis. NVAP is a new dataset and is a blending of TOVS, SSM/I, and radiosonde datasets from 1988 - 1992. NVAP is just now becoming available and the full 5 years are expected for release in summer 1995.

Figure 1 shows the regression relationship between the ERBE CS-OLR and NVAP Precipitable Water (or water vapor) for a 2x2 degree latitude-longitude box centered in the western Pacific. Daily OLR and WV pairs are plotted for all days in July 1988. The slope of the regression, or sensitivity, equals -1.13 which shows that for this area the OLR decreases 1.13 Wm^{-2} for each millimeter of WV.

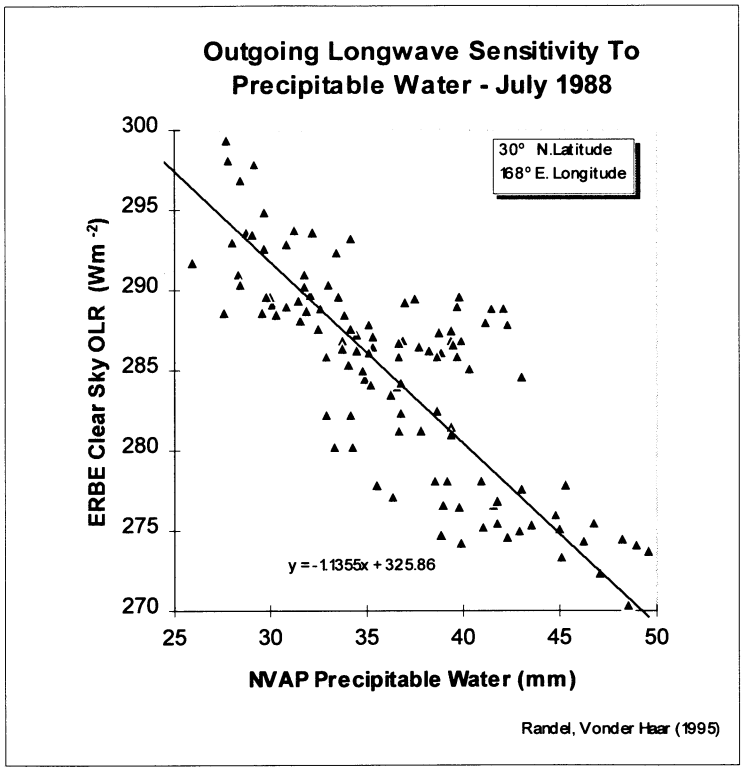

Figure 1. If statistically significant the best-fit regression line defines the OLR sensitivity to water vapor for a given 2x2 degree global grid box.

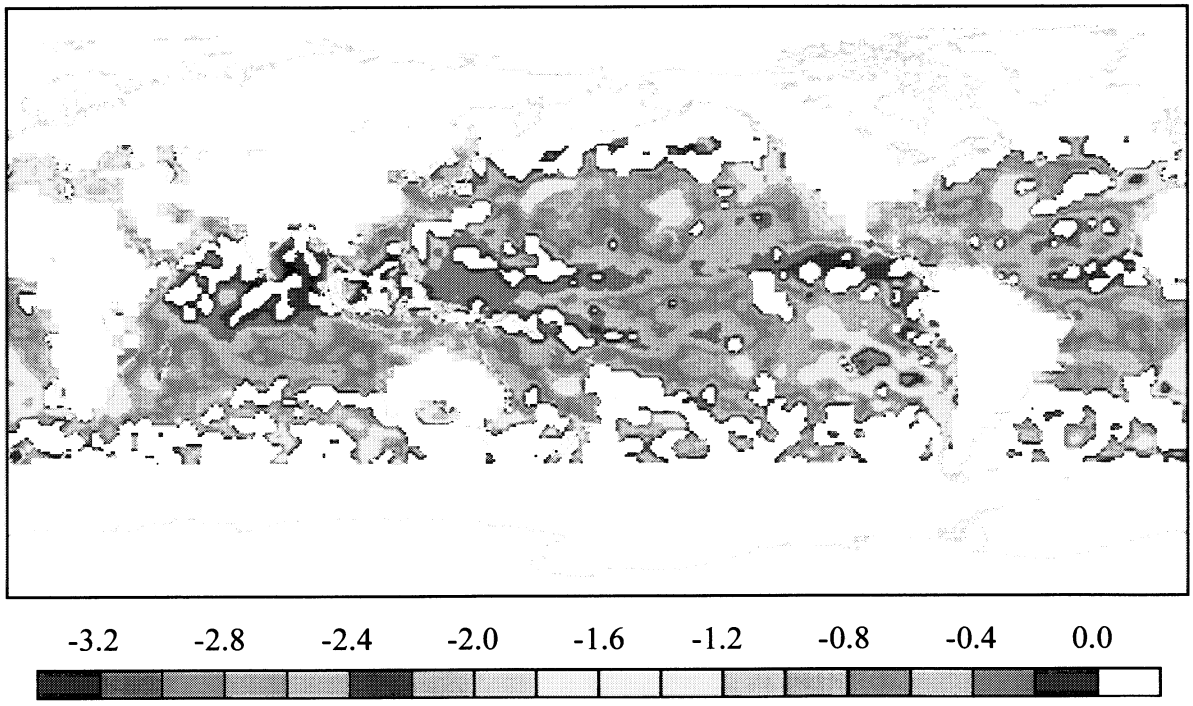

Figure 2. The sensitivity of the OLR to changes in water vapor for July 1988. Decrease in Clear-sky OLR per mm of PWC. (Wm^{-2} / mm)

By creating this regression for all gridpoints we can derive a geographical representation of the water vapor sensitivity and example of which is shown in Fig 2. The area of maximum sensitivity is off the west coast of South America. At first, this was thought to be caused by changes in the persistent stratocumulus found in this area. Spencer (1995) remarked that this area is where the global minimum in upper tropospheric water vapor or relative humidity is found. Since we know that changes in upper level water vapor have a large radiative effect on the OLR, it is felt that the high sensitivity in this area is caused by changes in upper tropospheric water vapor.

The y-intercept of the line in Fig. 1 equals 325.86 Wm^{-2} and represents the OLR with no water vapor in the atmosphere. Unlike the calculation of cloud radiative forcing, where by definition the clear-sky OLR occurs when there are no clouds, the PWC never is zero. Therefore one must make certain assumptions about the minimum level of PWC measurable for a given area. For many of the tropical pacific areas this minimum doesn't occur each year since the ENSO events modify the areas of convection and subsidence drying. Therefore, to define the minimum PWC for each gridbox, we used four years of NVAP daily PWC from 1988 - 1991 as shown in Figure 3. The Water Vapor Radiative Effect (WVRE) can then simply be defined as:

$$WVRE = (WV_{observed} - WV_{minimum}) * Sensitivity$$

There are ERBE problems that effect the ability to calculate a significant relationship of OLR to WV. These are mainly involved with using the ERBE daily CS OLR fields. Over land areas, which experience strong diurnal fluctuations in heating, the ERBE observations are inadequate to accurately describe the diurnal cycle and thus no daily averaged clear-sky OLR is produced. This leaves most continental areas without daily observations and limits the current study to primarily ocean areas. In addition the regression relationship does not always produce a significant correlation and these areas are eliminated. Due to an inadequate number of clear sky observations during the month, significantly cloudy areas over the ITCZ and monsoons regions produce insignificant correlation as well. Also since the regression depends on the surface emitting temperature remaining fairly constant throughout the month, highly variable polar latitudes are not used. Therefore in summary, global maps of WVRE using this technique have values primarily in tropical regions, over the oceans, and without persistent day-to-day cloudiness.

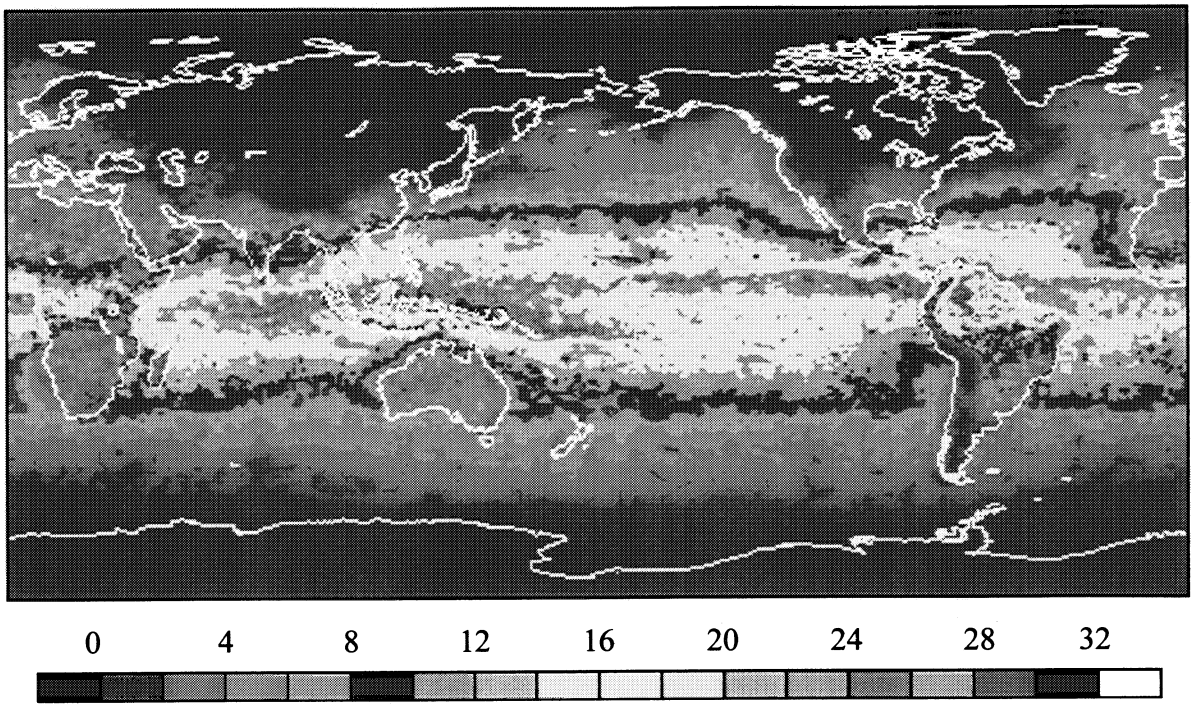

Figure 3. Minimum water vapor from the NVAP blended dataset (radiosonde, SSM/I, and Radiosonde) for the period 1988 - 1992 (mm). This is used as the minimum water vapor field in the water vapor radiative effect calculation.

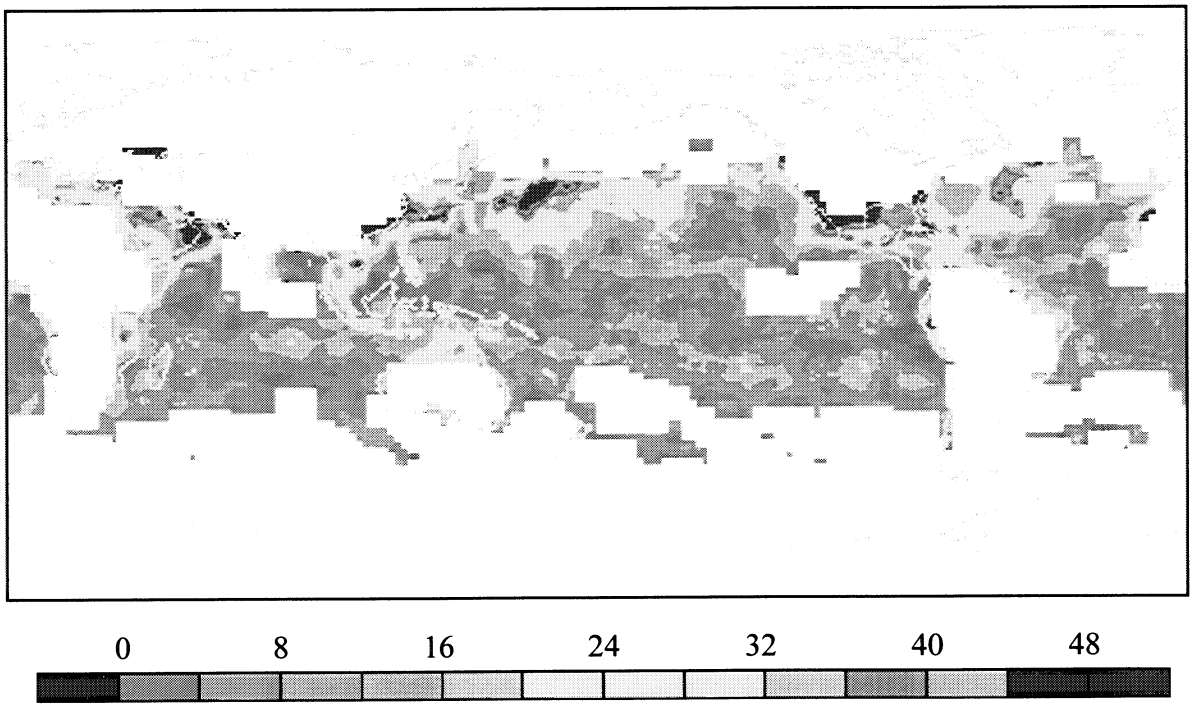

Figure 4. Water vapor radiative effect for July 1988. (Wm^{-2}).

Figure 4 represents the WVRE for July 1988. The predominately clear subtropical areas show the highest WVRE with annual values greater than 30 Wm^{-2}. This is comparable with the cloud radiative forcing which usually peaks near 50 Wm^{-2}. The seasonal cycle of WVRE is shown in Figure 5, the zonal average plots for the summer and winter months:

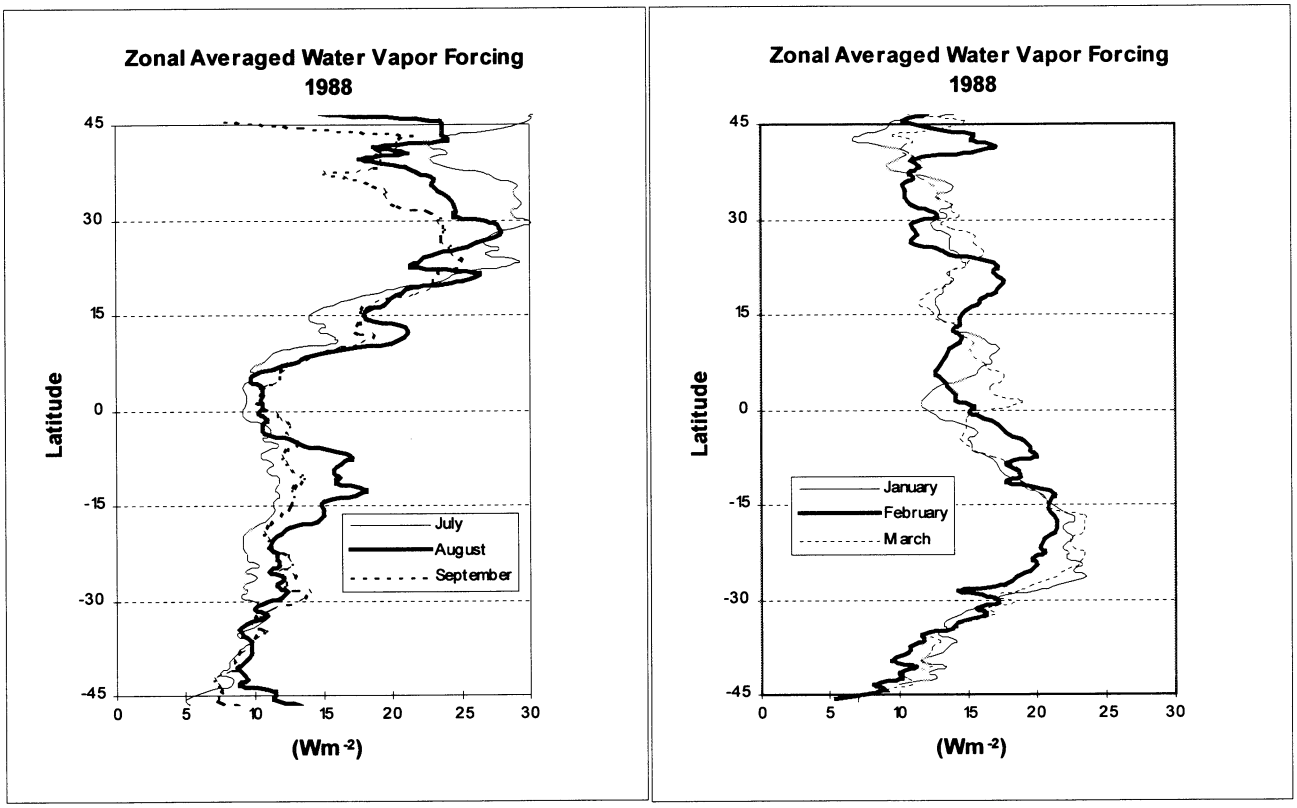

Figure 5. The zonal averaged water vapor radiative effect by season.

There is still much work to be done to fully understand the variability in the regression sensitivity. This will include using a radiative transfer model such as LOWTRAN to study the effects of differing water vapor profiles. Certainly the vertical distribution of the total PWC can have a large effect on the WVRE. We see some evidence of this in the sensitivity over stratocumulus regions where the PWC is limited to lower layers only and subsidence drying aloft is the norm.